

ELECTROHYDRODYNAMIC ACTUATORS ON A SUBSONIC AIR FLOW AROUND A CIRCULAR CYLINDER

Guillermo Artana*, Guillermo DiPrimo†, Eric Moreau‡, Gérard Touchard§

ABSTRACT

This work analyses the ability of an electrohydrodynamic actuator to modify the characteristics of an airflow around a circular cylinder. We analyze the flow regimes characterized by transition to turbulence of the shear layers and concentrate our analysis in the displaced and near wake regions.

We have considered a device consisting of electrodes flush mounted on the surface of the cylinder. The electrodes are excited with d.c. power.

This system is operated in a regime that gives rise to a plasma sheet contouring the cylinder which changes the boundary condition of the flow.

From flow visualizations and particle image velocimetry data we show that it can induce a strong acceleration of the flow close to the surface, leading to a decrease of the size of the near wake.

INTRODUCTION

The control of the wake produced by a bluff body has four major areas of significance:

- Drag reduction (a problem associated with energy consumption)
- Vortex shedding suppression (a mechanical or acoustical problem)
- Heat transfer enhancement (again an energy consumption problem)
- Wake dissipation (a problem associated with the signature on the fluid wake produced by a mobile body)

To enhance the control of these phenomena different strategies have been proposed. They can be gathered in two large groups:

One strategy consists in modifying the medium itself. Here we can find devices like those that alter the density field through heat transfer, the turbulence level of the incident flow, the composition of the media by the use of additives, etc.

The other strategy involves the use of actuators which try to perturb the flow by means of different mechanisms acting directly on the bluff body. We can consider here active systems (involving an energy transfer to the flow) like those using vibrations of the wake-producing body, or others devices close the body, sinks or sources of mass located on the surface of the body, or passive systems (no energy added) like compliant surfaces, surface roughness patrons, Scruton spirals, etc.

With some of the active devices it is possible to achieve either a static control (non time dependant) or a dynamic one (with variable frequencies, amplitudes and signal forms) of the near or far wake regions.

The kind of control that may be proposed depends primarily on the flow stability characteristics. As the near or far wake regions have in general different stability characteristics, the actuator excitation should be selected depending on the region where major effects are desired.

For near wake flows only static control has been proposed, since the instability in this region is usually absolute and this inhibits the use of a periodic excitation. On the other hand the far wake regions are normally convectively unstable and can support periodic excitation.

In this article we are interested in the possibility of controlling the near wake region, hence only a static control actuator will be considered.

*Professor, Department of Mechanical Engineering, Faculty of Engineering, University of Buenos Aires, CONICET, Buenos Aires, Argentina.

† Engineer, Department of Mechanical Engineering, Faculty of Engineering, University of Buenos Aires, Buenos Aires, Argentina.

‡Maitre de Conférences, Laboratoire d'Etudes Aérodynamiques (UMR 6609 CNRS), University of Poitiers, Poitiers, France

§Professor, Laboratoire d'Etudes Aérodynamiques (UMR 6609 CNRS), University of Poitiers, Poitiers, France

Most of the previous research has dealt with two principal methods to statically control the near wake flow. The first method concerns a splitter plate or a base bleed (steady blowing or suction at the base of the body) that try to modify the vortex shedding by uncoupling the phenomena between both sides of the cylinder. The second method tries to modify the flow field such that the conditions for absolute instability are changed and the flow becomes convectively unstable. Devices based on heating or cooling the surface or adding vorticity with a tripping wire are comprised in this group.

The devices proposed in both groups seem to be rather limited to low and medium Reynolds number and so they can be technologically questionable in most engineering domains¹.

As a result it seems necessary to try to excite the flow by other means in order to surpass some of the barriers previously found.

Recently, the use of actuators based on electromagnetic forces has been receiving special attention. They have important advantages like simplicity and reliability (they have no moving parts) and a very short response time (lower than 1 ns).

When currents involved are so low that the magnetic effects may be disregarded these devices are named electrohydrodynamic (EHD) actuators.

The use of EHD actuators in a gaseous media requires in most cases the creation of charged particles (ions) to materialize an electric force on the electrically neutral fluid. Ions can be created and injected in a dielectric fluid flow by means of an electrical discharge. These ions under the action of coulombian forces will drift, exchanging momentum with the fluid particles.

If in wall bounded or wake flows their trajectory takes place close to the wall, they can introduce changes in the fluid layers close to the surface where inertia forces are not so important. So, uniform discharges of low intensity concentrated in this region could largely modify the boundary conditions and hence the fluid flow field.

Prior research concerning EHD actuators has focused in different possible applications like shock wave control in hypersonic vehicles, heat transfer augmentation, or drag reduction²⁻¹³.

Some of the systems proposed, like the one of Malik and Bushnell¹⁰⁻¹¹ considered a system with needle points placed at the wall surface. This made possible to increase the air momentum mainly in the direction of the normal to the surface, without mass addition. As a result the longitudinal momentum could be reduced and boundary layer separation could be controlled. Although first results were promising research with this device has not been pursued probably because of the poor efficiency of the system in transforming electrical to mechanical energy at high Reynolds numbers.

Other devices with electrodes placed flush-mounted on the surface and momentum added to the fluid tangentially to the wall have recently been developed. Two different concepts of devices based on this idea are being studied.

Roth¹⁴⁻¹⁵ proposed devices based on a surface-generated atmospheric radio frequency (RF) plasma. The device named One Atmosphere Uniform Glow Discharge (OAUGDP) uses two electrodes separated by an insulating surface that avoids the knocking of the ions on the cathode, preventing the heating of it and the formation of new avalanches or breakdown from electron secondary emission. The authors claim that parraelectric forces associated to electric field gradients enable ion acceleration, and via particle collision, acceleration of the neutral particles. Other devices like the OAUGDP but with a polyphase RF power have been presented recently¹⁶⁻¹⁷.

The second kind of devices uses a different approach as electric forces are mainly coulombian. It consists on two electrodes flush mounted on the same side of an insulating surface which create a bipolar corona with a d.c. voltage excitation.

Recent results¹⁸⁻²⁴ indicate that this device can be operated in a special discharge regime characterized by the formation of a plasma sheet contouring the surface. The operation in this regime avoids problems of non-uniformities along the electrodes and changes drastically the boundary condition at the wall.

Though some similarities exist with the needle points placed at the wall, this kind of actuator seems a better candidate to obtain good efficiency in transforming electrical into mechanical power.

Two main differences are the basis of this assertion. First, the action with this actuator is uniform around the body and not only in discrete points.

The other is linked to the region where the electric forces take place. With this device the ions drift under the action of a designed electric field configuration. By doing this it is possible to transfer momentum to fluid particles that are far from the regions where inertia forces are important and where electric forces will have very low incidence.

In this article we are interested in analyzing the capability of these devices to control the flow around bluff bodies.

We will analyze a body of circular section as this flow type is usually considered a prototype flow for more general bluff bodies.

Of the different regions of this flow that can be controlled we will concentrate only on the near wake region. The goal of this work is to try to identify if in this configuration the ion-fluid particle interaction is high enough to modify the characteristics of the flow in this region. The flow regimes that will be analyzed are those characterized by the transition to turbulence of the shear layer, regime that is often encountered in mechanical, chemical and nuclear engineering applications.

EXPERIMENTAL SETUP

In our study the injection of ions in the fluid is obtained by means of a d.c. voltage excitation of a wire electrode (0.90 mm diameter) and a plane electrode of aluminium foil. These electrodes are located flush-mounted on the surface of a cylinder of PMMA (32 mm diameter) and disposed parallel to the cylinder axis as shown in Figure 1.

Two different H.V. sources of opposite polarity (+20kV, -20kV, 1.5 mA) are used to impose a voltage difference between both electrodes high enough to sustain a stable discharge.

The wire type electrode is connected to the positive polarity source and the plate electrode to the negative one. By increasing the voltage difference between both electrodes different discharge regimes can be established. The current measurement is undertaken with an electrometric circuit which can detect currents of 1 nA (Figure 2).

Visualizations at low velocities have been done with the cylinder placed in a wind tunnel (0-5 m/s, 0.28 x 0.28 m² rectangular cross section) with the axis horizontal and parallel to the main flow. The wire electrode was facing the flow in the frontal stagnation point.

Visualizations has been done with a smoke injection technique. The device comprised a laser sheet produced by a 5W argon-ion laser and a single smoke filament ($\phi=2\text{mm}$). Seeding was produced with a smoke generator EI 514 Deltalab that uses a pure cosmetic grade oil. It was operated to obtain a cloud with a mean particle diameter of 0.3 μm . Images have been recorded with a videocamera and then digitalized.

Particle image velocimetry (PIV) measurements have been done in a closed wind tunnel (2-30m/s, rectangular probe section of 0.50x0.50m²). The cylinder was placed in the probe section as in the tunnel used for flow visualization experiments

The experiments have been conducted using the DANTEC system controlled by FlowMap® PIV. Interrogation area was 32 x 32 pixels with an overlap of 50 %. Seeding was also done with particles of a pure cosmetic grade oil like in the visualization experiments and with the same mean diameter.

The system was illuminated with a laser sheet produced by a Yag laser of 200mJ. In our experiments each pulse had a duration of 0.01 microseconds and the time between a pair of pulses was 50 microseconds. The progressive scan interline camera we have used can produce images of 768 x 484 pixels. We considered in each experiment 400 pairs of digital images taken every 0.1s.

EXPERIMENTAL RESULTS

Discharge Characteristics

A typical voltage-current curve is shown in Figure 3. In our experiments the different regimes we could observe are similar to those described in previous works¹⁸⁻²².

A first regime correspond to the first part of the curve with very low currents (lower than 0.2 $\mu\text{A/m}$). In this regime the corona discharge is almost negligible. This regime occurs for voltage differences lower than a value close to 25 kV. At higher voltage differences other regimes occur that have the following characteristics:

Spot type regime: (Figure 4) The discharge is concentrated in some visible spots of the wire and by increasing the voltage difference they can increase in number. Some of them may ionize in a plume-like type or may lead to a narrow channel quite attached to the surface. In Figure 3 this regime corresponds to the range of currents lower than 0.1 mA/m and voltage differences lower than a value close to 30 kV.

Generalized glow regime: (Figure 5) At higher voltage differences, a regime characterized by a homogeneous luminescence can be observed. In Figure 3 this regime corresponds to voltage differences of about 30-35 kV and currents between 0.5-1.1mA/m. This kind of discharge is quite homogeneous, noisy and the current quite stable with time. The luminescence occupies the whole interelectrode region and makes the cylinder look like supporting a thin film of ionized air. By visual inspection it appears that

the thickness of the ionized film is of the order of the thickness of the aluminum foil (50 micrometers). The discharge is largely dependent on the quality of the finishing of the electrodes. Sometimes it is hard to start and it can be promoted by blowing towards the plate surface hot air produced with a hair drier. In the range of our experiments (1-30m/s) the intensity of the current of the discharge is not significantly modified by the velocity of the flow of air.

Filament type regime: (Figure 6) By further increasing the voltage differences a regime that precedes immediately the air breakdown (sparks) can be observed. Some points of the wire have a concentrated discharge in an arborescent shape of the filament type that lead to some localized sparks following a trajectory at a small distance from the surface.

In the present work we have undertaken the flow measurements in the generalized glow regime.

Flow Visualization

Figures 7 and 8 are photos showing typical visualizations at low velocity ranges ($V \approx 1\text{m/s}$). They show two sequences obtained from different position of smoke filament. These sequences enable to observe the evolution of changes of the smoke tracers at different times prior (Figures a) and after the electric field is applied at time $t=0$ (Figures b). The wire electrode is placed on the frontal stagnation point (at left in the photo) and the plate electrode is opposed (at 180 degrees).

PIV data processing

Each velocity field has been filtered with a peak-validation and a range validation filter. Peak validation filter is based on the detectability criterion²⁷ which validates vectors with a ratio of the highest peak to the second highest peak in the correlation plane larger than a fixed value (1.2 in our case). The range validation filter enables to establish the range admitted for the modulus of the velocity vectors. In our case we have considered a maximum value of 2.5 of the flow velocity U_0 as the upper limit. Undertaking these filtering processes, about 5% to 10% vectors are removed from the 1363 initial vectors.

In one experiment an average over 400 vector fields is performed in order to obtain a mean velocity field of the airflow.

We show typical results concerning to this mean velocity field in Figures 9. These figures correspond to $Re \approx 35600$. We also show contour and vector diagrams of the difference between the averaged velocities with electric field on and off (Figures 10-11) to highlight the differences in flow.

Even when vortices are shedding, it is possible to define a "mean recirculation region" by averaging over a large time (compared to the shedding period). This region is symmetric and closed and is characterized by a bubble length (L_b) and bubble width (Db) distance. A measure of the length of such region is given by the eddy formation length (L_f) defined by the distance downstream from the cylinder axis to the point where the rms velocity fluctuations are maximized on the wake center line.

Figures 9 make clear the mean recirculation region without the use of this concept.

DISCUSSION

Physical interpretation of the electrical results

In a previous work¹⁸ we have analyzed the electric field configuration that occurs in a device with electrodes flush mounted on a dielectric cylinder as the one proposed in this article. In the model considered we have taken into account the effect of surface conductivity of the dielectric by considering as a boundary condition that the electric potential on the cylinder surface between electrodes has a linear decay with the angular coordinate. Under this assumption it is easily demonstrated that the electric potential is

$$\phi = \frac{4 V_1}{\pi^2} \sum_{n=1}^{\infty} \left(\frac{a}{r} \right)^n \left(\frac{(-1)^n - 1}{n^2} \right) \cos(n\theta) + V_2 \frac{\ln(r/R_{\infty})}{\ln(a/R_{\infty})}$$

where a is the cylinder radius and R_{∞} is the distance to earth in our case the distance to the walls of the probe section and V_1 and V_2 are linked to the electrode potential ϕ_1 and ϕ_2 by

$$2V_1 = \phi_1 - \phi_2; \quad 2V_2 = \phi_1 + \phi_2$$

Considering this expression it is easily seen that it leads to a large concentration of the electric field occurring in the vicinity of the cylinder surface. As a result when electrodes are disposed flush-mounted on the surface in planar or cylindrical geometries the electric field configuration close to the surface has large similarities, and so one would expect large similarities in the discharge behavior which occurs.

Different researchers²⁵⁻³¹ have considered devices with electrodes flush-mounted on the surface of a dielectric plate in laser research. An important difference with our device is that in most cases the electrodes were excited with a pulsed voltage difference. Also a grounded electrode was placed in the reverse side of the plate.

The different discharge regimes for this pulsed excitation were described by Baranov et al^{28,31} and surprisingly they are quite similar to the ones we have observed with the d.c. excitation.

It has been observed that at a certain range of voltages and depending on specific conditions of the experiments, a uniform luminosity like a plasma sheet covering the space between both electrodes takes place. This phenomena has been reported with different names like sliding discharge, grazing discharge or skimming discharge.

Rutkevich^{30,31} proposed a model of a stationary wave of ionization to describe the propagation of this discharge. This model predicts typical results of the plasma sheet between 0.1-1mm, apparently quite close to the one we can observe in our device.

The similarities that exists between both processes, the pulsed voltage case and the d.c. voltage case, seems to indicate that both phenomena have the same origin. Then, presumably the generalized glow regime that leads to a uniform plasma sheet though produced with a d.c. excitation should be a pulsating discharge.

Considering that repetitive streamers regimes produced with electrodes excited with d.c. voltages lead also to pulsating discharges³²⁻³³, this first approach appears justifiable.

The scenario should then be a repetition of ionization waves, each front of ionization screening the electric field and impeding the formation of a new discharge until the neutralization of the effect of the front. The promotion of the plasma sheet by the use of hot air seems also to be associated, like in point to plane repetitive streamers, with the creation of lower density air channels³³.

However, in order to corroborate the model proposed and fully describe the phenomena, further experiments should be undertaken and the use of a refined model to describe pulse propagation is still needed.

Finally, from our experiments it can be observed that typical values of power consumption per unit area associated with the plasma sheet are about 500W/m². They are similar to those needed to sustain a glow discharge with the OGADUP device and to those obtained with similar EHD actuators in a planar configuration.

Fluid mechanics results interpretation

In flow visualization by smoke injection techniques or PIV experiments, the trajectories of the seeding particles and those of the fluid particles surrounding the tracer are usually considered the same.

When there is a slipping velocity between the tracer and the fluid the trajectories differ. The tracer particles “swim” in the moving media and information obtained from the tracer must be carefully examined.

Hinze’s model³⁴ gives an expression that enables to establish the particle size to track properly the flow and to avoid this problem, based on the following equilibrium equation

$$\frac{\pi}{6} d_p^3 \rho_p \frac{d\hat{U}_p}{dt} = F_{st} + F_p + F_f + F_u$$

F_{st} describe the viscous drag as given by Stokes law, F_p is the pressure gradient force, F_f takes into account the resistance of an inviscid fluid to acceleration of the seeding particle and F_u is the Basset history integral that represent the drag force associated with unsteady motion.

The formula is valid under different assumptions that are usually verified (low particle density, particles are spherical,...) but in our case one of the strongest is that the model considers that electrostatic forces are negligible. If we neglect this effect we could introduce errors in the analysis. In our case it may be argued that some smoke particles can be charged by ion impact and coulombian forces would act on them affecting tracer’s trajectory.

In a previous work²¹ we have analyzed this phenomena and established that the ratio of the Stokes force to the electrical one (F_{el}) is given for a non polar hydrocarbon seeding particle by

$$\frac{F_{st}}{F_{el}} \approx -\frac{3\pi\mu d_p}{1.5\pi d_p^2 \varepsilon_0 E_0^2} (U_p - U_f)$$

with μ the coefficient of dynamic viscosity, ε_0 the Faraday constant and E_0 the electric field. We see in this expression that the influence of the electric forces is negligible when the seeding particle diameter (d_p) is very low.

For instance when considering an air flow and an electric field $E_0 \approx 10^6$ V/m the largest size of the tracer should be limited to particles of about $1\mu\text{m}$.

Considering the data sheet given by the constructor of the smoke generator, in our experiments, the seeding particles we have used are in the range of $0.3\mu\text{m}$. So, in our PIV and visualization experiments the influence of coulombian forces on tracers trajectory in a first approach can be disregarded.

Flow visualization

Flow visualization by smoke injection technique gives an idea of the effect of the discharge in the flow field.

Without electric field Zdravcovich³⁵ has proposed a classification of the different flow regimes around a circular cylinder as a function of Reynolds number. Considering this classification our flow visualization experiment has been undertaken in the regime of intermediate subcritical regime of transition in shear layer state ($1-2k < Re < 20-40k$). The near wake in this state of flow is surrounded by initially laminar free shear layers. However as Re increases this regime shows undulations in the shear layer (transition waves) that roll up into discrete eddies (transition eddies) along the free shear layer before becoming turbulent. The transition region may move with increasing Re along the free shear layer towards the separation region and affects the length and width of the near wake.

The sequence of Figures 7 shows how the electric field changes the pattern of the flow on one side of the displaced or accelerated flow. We observe that after a short period of time the non perturbed flow region disappears from the image. Then the smoke filament indicates an important acceleration of the fluid layers close to the cylinder surface. As a result a drag of other fluid layers is produced and a pumping of fluid from the central region is produced that finally lifts the smoke filament.

The sequence of Figures 8 reveals the effect of the actuator on the separated shear layer and on the near wake. We can see that after a small period of time a new flow condition in the near wake is established. The separated shear layer seems closer and the eddy formation region is largely perturbed. The pictures show that in the image field vortex streets can no longer be detected.

This intense effect is greatly reduced if the discharge operates in other regime (spot or filament type). There the 2-D character of the flow is lost and the coincidence of the discharge channels with the region of interest (the plane of visualization) is sometimes very difficult.

Particle Image velocimetry

We considered larger flow velocities in PIV experiments than those of visualization by smoke injection. The results we show are typical ones that have been obtained at flow velocities of 16.7 m/s ($Re \approx 35500$). Similar results can be obtained in the range of present experiments ($10-20$ m/s). Considering Zdravcovich's classification these experiments have been conducted in the lower part of the upper subcritical regime of the transition in the shear layer state ($20-40k < Re < 100-200k$). The regime is characterized by an almost immediate transition to turbulence of the separated shear layer that is accompanied by a very short near wake region almost constant in size in all the Re range of this regime. The suction base pressure coefficient C_{pb} , the drag coefficient C_d and the Strouhal number St are also almost independent of Re number in this regime.

Figures 10 shows the effect of the actuator in the accelerated region close to the separation. In this figure we analyze the resulting velocity field from the difference between the cases with voltage on and voltage off.

We can see there that the actuator produces an important acceleration of the fluid layers close to the cylinder surface. Maximum differences can attain values of 8.5 m/s (about half of the incident flow velocity).

Velocity profiles at different angles can be deduced from these velocity fields and are shown in Figures 12. We show results close to the separation line for angles $80^\circ-85^\circ-90^\circ-95^\circ$ (at the frontal stagnation point the angle is null). Important changes on the shape of the velocity profiles can be seen close to the cylinder surface and larger changes can be observed at the layers closer to the cylinder. This effect becomes more important as we consider the larger angles.

This can be explained if we consider that the actuator introduces momentum changes on the boundary layers that are subjected simultaneously to diffusion (mainly in the direction of the normal to the surface) and convection processes (mainly in the flow direction). As a result at positions closer to the frontal stagnation point, the streamlines

that are far from the surface “feel” less what happens at the boundary than those closer to it. As we consider positions at larger distances from this point, diffusion modifies the momentum of the less perturbed layers (those far from the surface) and the velocity profile modifications penetrate more in the fluid.

We observe in Figures 9 and 11 the effect of the actuator on the near wake and on the separated shear layer.

Employing the concept that the pressure and the shear stresses on the recirculation bubble are in equilibrium it is easily demonstrated that there is a link between the bubble length and the base pressure³⁶⁻³⁷. In general a shortening of the bubble leads to an increase of the base suction pressure.

After the above mentioned data processing Figures 9 make evident the mean recirculation region. Looking carefully at these figures we can observe that the actuator provokes a narrowing and a shortening of it.

Figure 11 shows the subtracted velocity field. It reveals an important acceleration of the region close to the separated shear layer and shows the origin of this shortening and narrowing.

In the Re range considered this region in the non excited flow is fixed in size. The PIV data shows that the actuator is effective to modify it.

As a result of these changes an increase of the suction base pressure should be expected. In a previous work we show results concerning the mean pressure as a function of the angle. There an increase of the base suction pressure of about 20% for Re numbers close to 10 k has been detected.

So, the effects of the EHD actuator on the base pressure observed in the experiments undertaken at lower mean flow velocities are confirmed at larger Re numbers.

SUMMARY

The effect on the flow of the EHD actuator operating in the generalized glow regime is very distinctive because of two main factors :

- its intensity (luminescence in all the arc distance indicates the phenomena involves high momentum particles)
- its uniformity (the uniformity of the discharge occurs all along the electrode length and not in some isolated points).

We have undertaken our experiments in the flow regime around a cylinder identified by transitions of the shear layer (intermediate subcritical or upper subcritical regime).

Flow visualization experiments indicate that at relatively low Re number the effect of the discharge in the flow field close to the cylinder is very important. They reveal that the actuator can produce an important acceleration of the fluid layers close to the cylinder surface and an approach of the separated shear layer to the cylinder. The effect of the actuator seems very important in the near wake where vortex shedding is not clearly observed.

PIV measurements enabled us to corroborate that a relative strong acceleration of the fluid layers persists at larger Re number. This leads to a shortening and narrowing of the mean recirculation region and to an increase of the mean suction base pressure.

The EHD actuator proposed here seems to surpass the limitations of Re ranges of other flow control devices. An important control of wake flows may be expected to be attained with these actuators in larger ranges of Re numbers.

However experiments considering the static control proposed here but at larger flow ranges should be undertaken. Also the possibility of a dynamic control device to modify the eddy shedding and the far wake characteristics should be considered in a future work.

***Acknowledgements:** This research has been done with grants UBACYT AI-25 and PICT 12-02177 of the Argentine government*

We would like to thank the authorities of the University of Poitiers for inviting Prof. G. Artana to undertake this research with part of the staff of the Laboratoire d'Etudes Aérodynamiques.

REFERENCES

1. Flow control, Eds Gad-el-Hak M., Pollard A., Bonnet J.P., Springer Verlag NY-1997, pp 374-376.
2. Velkoff H, Kulacki F, “Electrostatic Cooling”, ASME paper No 77-DE-36, 1977
3. Kibler K., Carter G., “Electrocooling in Gases”, J. Appl. Phys, Vol 45, 1974, pp 4436-4439.

4. Ohadi M., Nelson D., Zia S., "Heat Transfer Enhancement of Laminar and Turbulent Pipe flow via Corona Discharge", *Intl. J. of Heat and Mass Transfer*, Vol 34, 1991, pp 1175-1187.
5. Noger C., Chang J. S., Touchard G., "Active Controls of Electrohydrodynamically Induced Secondary Flow in Corona Discharge Reactor" *Proc. 2nd Int'l Symp Plasma Techn. Pollution Cont, Bahia, 1997*, pp136-141
6. Vilela Mendes R., Dente J., "Boundary Layer Control by Electric Fields", *Journal of Fluid Engineering*, Vol 120, 1998, pp 626-629.
7. El-Khabiry S., Colver G., "Drag Reduction by D.C. Corona Discharge Along an Electrically Conductive Flat Plate for Small Reynolds Number Flows", *Physics of fluids*, Vol 9, No 3, 1997, pp 587-599.
8. Colver G., El-Khabiry S., "Modeling of DC Corona Discharge Along an Electrically Conductive Flat Plate with Gas Flow", *IEEE Trans on Industry Appl.*, Vol 35, No 2, 1999, pp 387-394
9. Soetomo F., "The influence of High Voltage Discharge on Flat Plate Drag at Low Reynolds Number Air Flow", M. S. Thesis, Iowa State University, Ames, Iowa, 1992.
10. Bushnell D., "Turbulent Drag Reduction for External Flows", AIAA-83-0231, Jan. 1983.
11. Malik, Weinstein L., Hussaini M., "Ion Wind Drag Reduction", AIAA-83-0231, Jan. 1983.
12. Cahn M., Andrew G., "Electroaerodynamics in Supersonic Flow", AIAA paper No 68-24, NY, Jan. 1968.
13. Sin-I-Cheng, Goldburg A., "An analysis of the possibility of Reduction of Sonic Boom by Electroaerodynamic Devices", AIAA paper No 69-38, NY, Jan. 1969.
14. Roth J. R., Sherman D., "Boundary Layer Flow Control with a One Atmosphere Uniform Glow Discharge Surface Plasma", AIAA paper 98-0328, Jan. 1998.
15. Roth J., Sherman D., "Electrohydrodynamic flow control with a glow discharge surface plasma, AIAA J., 38,7, 2000, pp 1166-1178.
16. Corke T., Mattalis E., "Phased Plasma Arrays for Unsteady Flow Control", AIAA paper 2000-2323, June 2000.
17. Lorber P., McCormick D., Pollack M., Breuer K., Corke T., Anderson I., "Rotorcraft Retreating Blade Stall Control", AIAA paper 2000-2475, June 2000.
18. Artana G., Desimone G., Touchard G., "Study of the Changes in the Flow Around a Cylinder Caused by Electroconvection", *Electrostatics'99*, IOP Publ. Ltd, Bristol-Philadelphia, 1999, pp 147-152.
19. Desimone G., DiPrimio G., Artana G., "Modification of the Flow Around a Cylinder by Means of Electrodes Placed on its Surface", *Proc. Colloque de la Societe Francaise d'Electrostatique, Poitiers, June 1999*, pp 80-84.
20. Desimone G., "Estudio experimental de la modificacion del escurrimiento alrededor de un cilindro circular a traves del aelectroconvección", *Tesina de Grado, Facultad de Ingenieria, Universidad de Buenos Aires, 2000*.
21. Artana G., D'adamo J., Leger L. Moreau E., Touchard G., *Flow control with electrohydrodynamic actuators, AIAA paper 2001-0351, January 2001*.
22. G. Artana, J. D'adamo, G. Desimone, G. Diprimio, *Air flow control with electrohydrodynamic actuators, 2nd Intl Workshop on Conduction Convection and Brakdown in Fluids, Grenoble, 190-194, May 2000*.
23. L. Leger, E. Moreau, G. Artana, G. Touchard, *Modification de l'ecoulement d'air autour d'une plaque plane par une decharge couronne, Colloque de la Societe Francaise d'Electrostatique, Montpellier, 97-101, June 2000*.
24. Leger I., *Influence d'une decharge couronne DC sur l'ecoulement d'air autour d'une plaque plane en incidence, Memoire DEA, LEA-Universite de Poitiers, 2000*.
25. Andreev S., Belousova I., Dashuk P., Zaruslov D., Zobov E., Karlov N., Kuz'min G., Nikiforov S., Prokhorov A., "Plasma-sheet Co₂ Laser", *Sov. J. Quantum Electron*, Vol 6, No 8, 1976, pp 931-934.
26. Dashuk P., Kulakov S., "Formation of an Electron Beam in the Plasma of a Skimming Discharge", *Sov. Tech. Phys. Lett*, Vol 7, No 11, 1981, pp 563-565.
27. Atanasov P., Grozdanov K., "Simultaneous Ultraviolet and Infrared Emission in a Sliding-Discharge Excited Laser", *IEEE J. Of Quantum Electronics*, Vol 32, No 7, 1996, pp 1122-1125.
28. Baranov V., Borisov V., Vysikailo F., Kiryukhin B., Khristoforov O., "Analysis of Sliding Discharge Formation", *Kurchatov Inst. Atom. Energy, N°3472/7, (in Russian), Moscow, 1981*.
29. Beverly R., "Electrical Gasdynamics and Radiative Properties of Planar Surface Discharge", *J. Appl. Phys.*, Vol 60, No1, 1986, pp 104-124.
30. Rutkevich I., "Structure of a Grazing Discharge Front", *Sov. Phys.-Tech.Phys*, Vol 31, No 7, 1986, pp. 841-842.
31. Lagarkov A., Rutkevich I., "Ioniztion Waves in Electrical Breakdown of Gases", Springer-Verlag, NY, 1993, pp 195-207.
32. Goldman M., Sigmond R., "Corona and Insulation", *IEEE Trans. On El. Insul.*, Vol 17, No 2, 1982, pp 90-105.
33. Sigmond R., Goldman M., "Positive Streamer Propagation in Short Gaps in Ambient Air", *Proc 15th Int. Conf. On Phenomena in Ionized Gases, Minsk, 1981*, pp 649-651.
34. Fuchs N., "The Mechanics of Aerosols", Dover, NY, 1964, pp 21-180.
35. Zdravcovich M., *Flow around circular cylinders, Oxford Science Pub, Oxford, Vol I, pp1-18, 1997*.
36. Williamson C., *Vortex dynamics in the cylinder wake, Ann. Rev Fluids Mechs, 28, pp 477-539, 1996*.
37. Roshko A., *Perspectives on bluff body aerodynamics, J Wind Ind Aerodyn, 49, pp 79-87, 1993*.

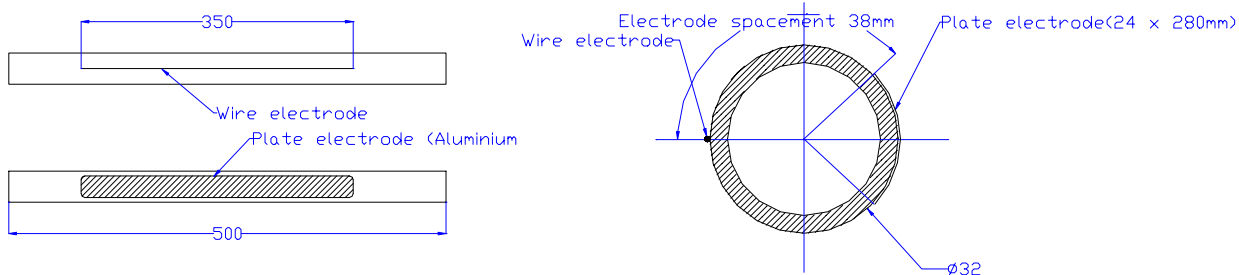


Figure 1: Schematic of the Electrode configuration

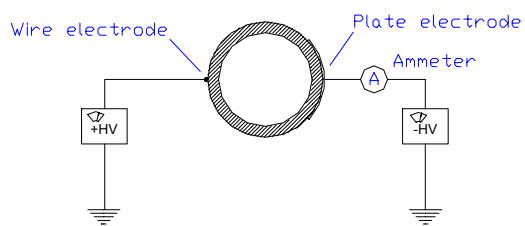


Figure 2: Schematic of the electric circuit

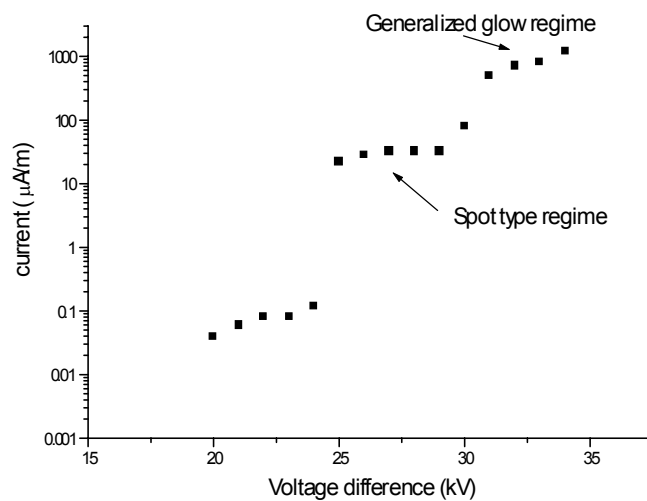


Figure 3: Voltage-current curve

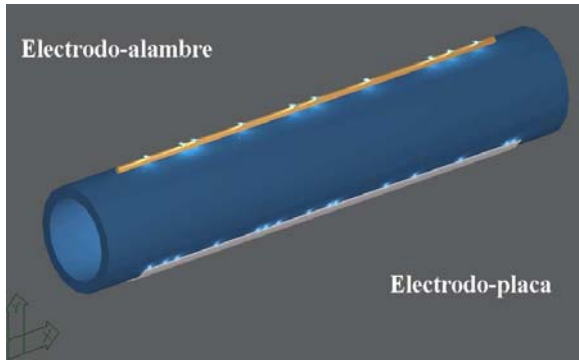


Figure 4: Scheme of the Spot regime

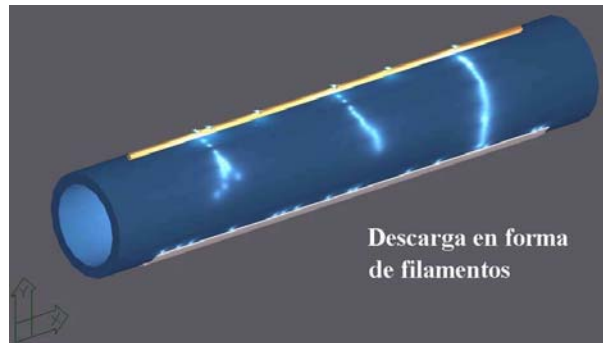


Figure 6: Schematic of the filamentary regime

Figure 5: Photo of the Generalized Glow

Figure 7a) $T=-0.04s$

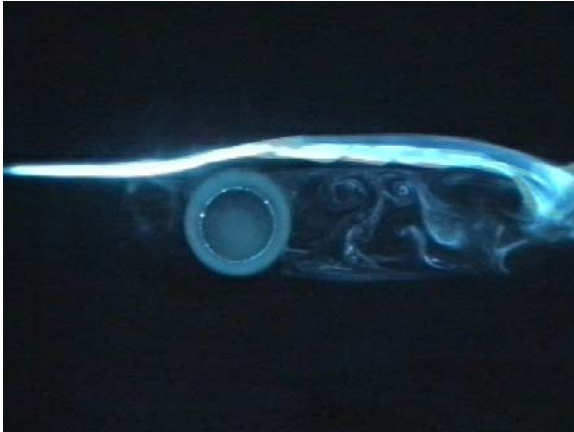


Figure 7b) $T=0.00s$ (electric field on)

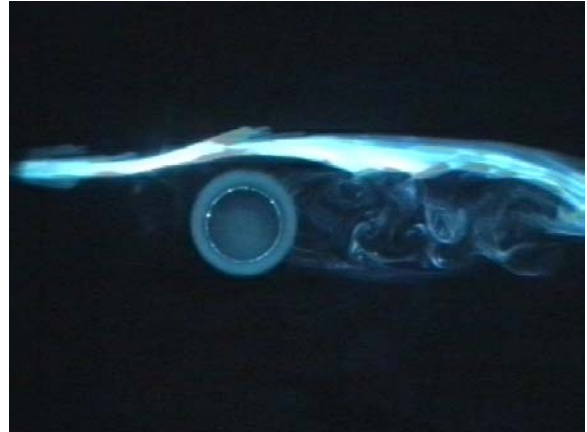


Figure 7c) $T=0.04s$

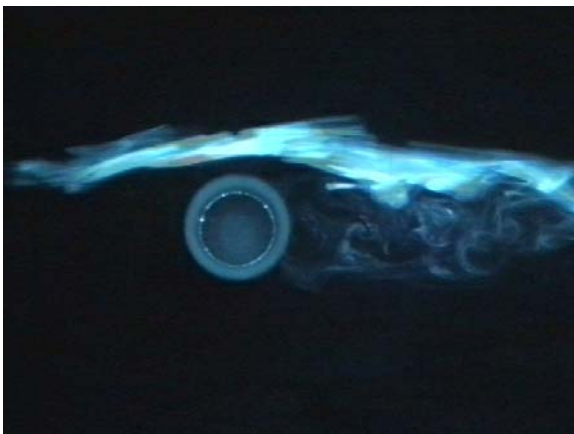


Figure 7d) $T=0.08s$

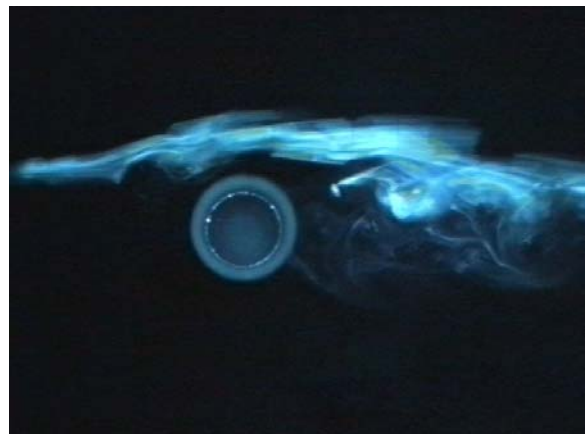


Figure 7e) $T=0.28s$



Figure 7f) $T=0.48s$



Figures 7: Sequence of visualizations when applying the electric field at time $T=0.00s$. $U_0=0.7m/s$. $\Delta\phi=32kV$

Figure 8a) $T=-0.04s$

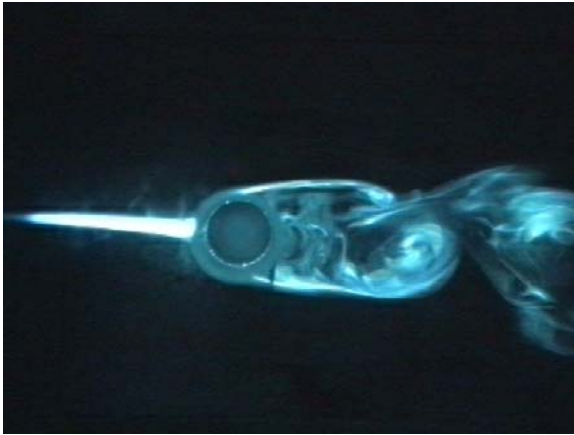


Figure 8b) $T=0.00s$ (electric field on)



Figure 8c) $T=0.04s$

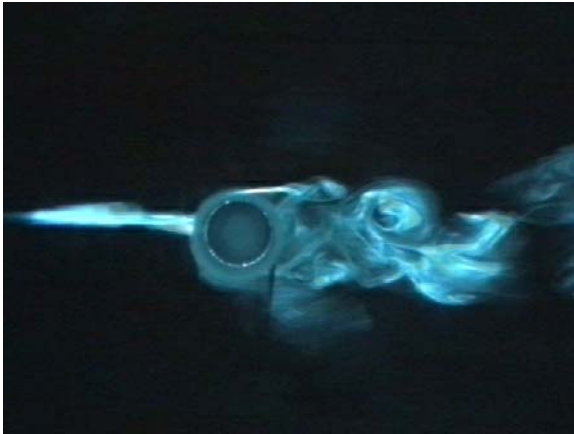


Figure 8d) $T=0.12s$

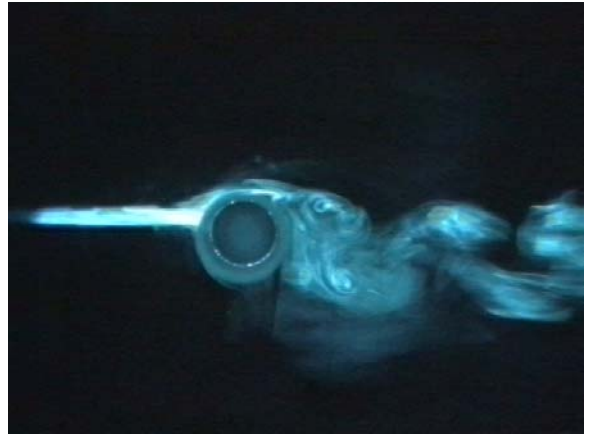


Figure 8e) $T=1.56s$

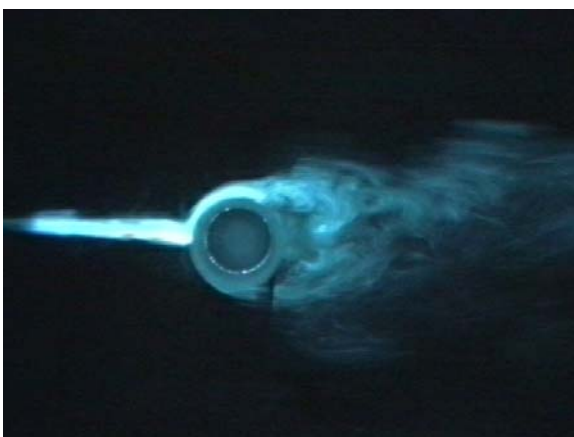
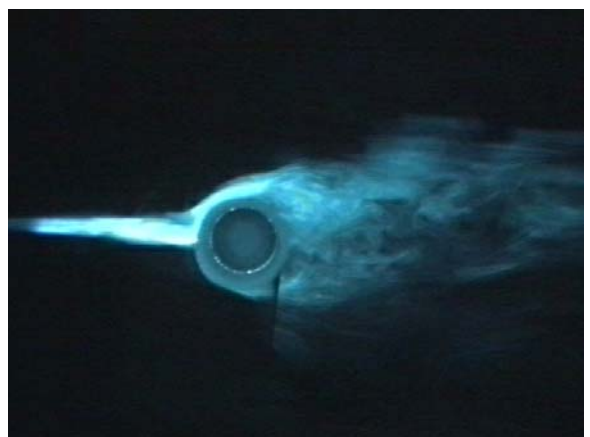


Figure 8f) $T=1.60s$



Figures 8: Sequence of visualizations when applying the electric field at time $T=0.00s$. $U_0=0.7m/s$. $\Delta\phi=32kV$

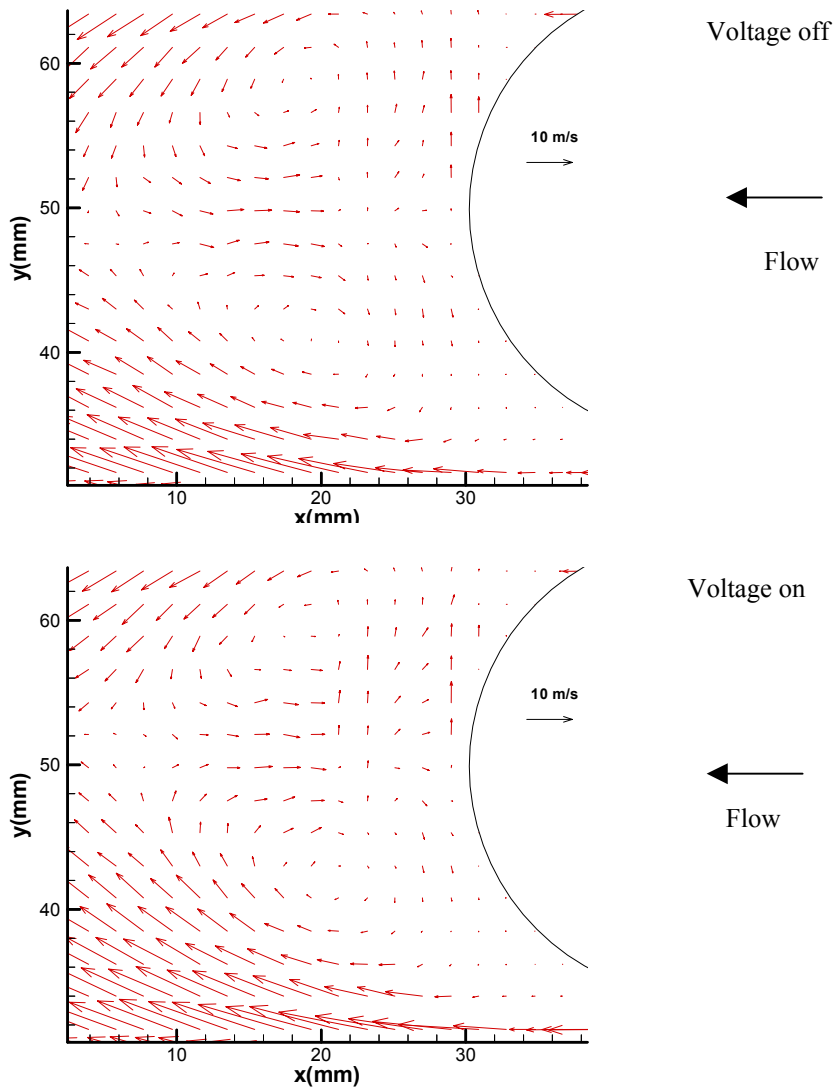


Figure 9: Velocity field in the near wake- $U_0=16.7\text{m/s}-\Delta\phi=34\text{kV}$

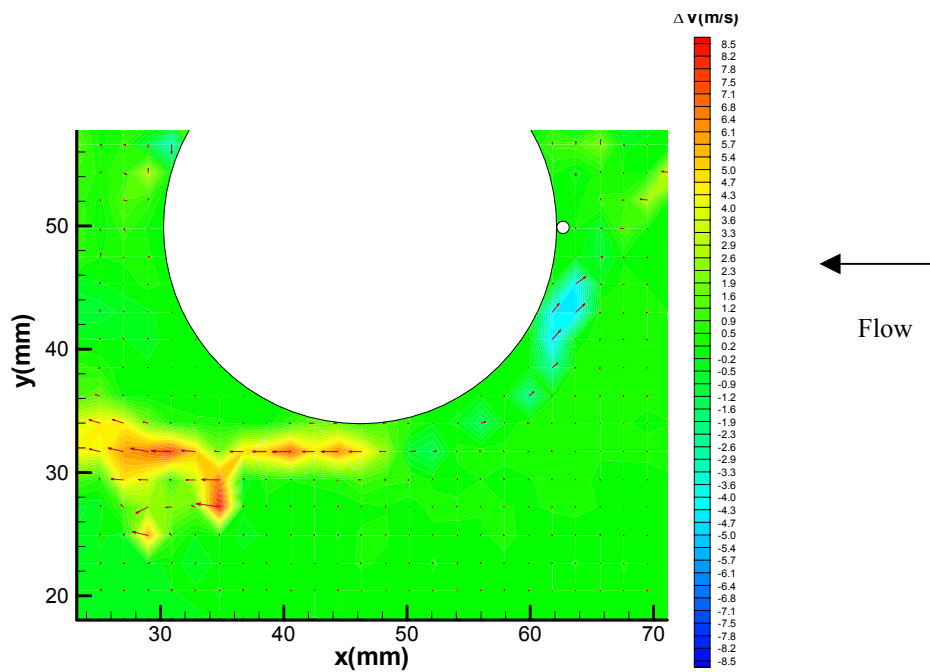


Figure 10) Velocity field difference in the displaced region- $U_0=16.7\text{m/s}-\Delta\phi=34\text{kV}$

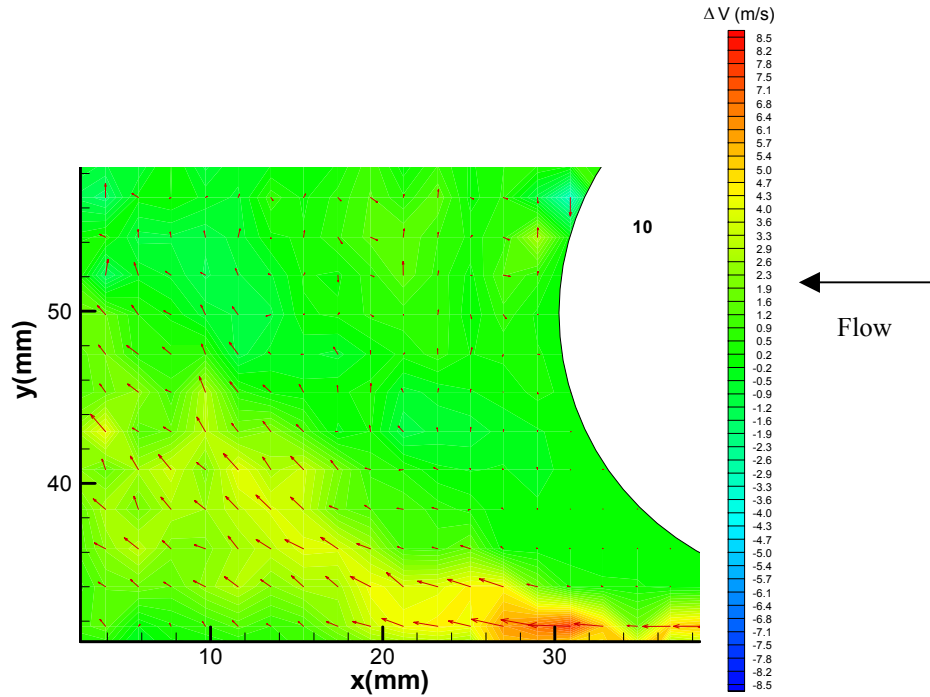


Figure 11) Velocity field difference in the near wake region- $U_0=16.7\text{m/s}-\Delta\phi=34\text{kV}$

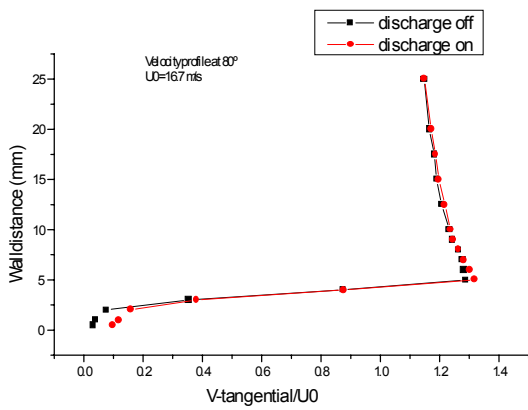


Figure 12a)

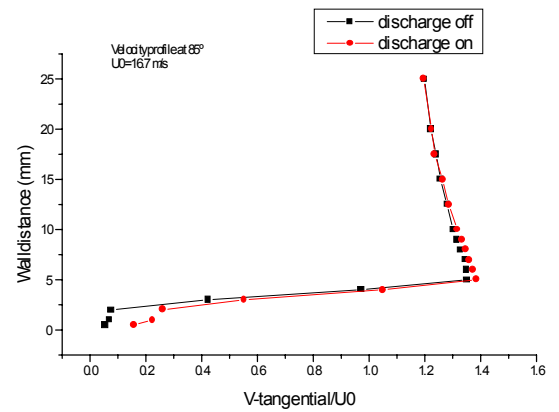


Figure 12b)

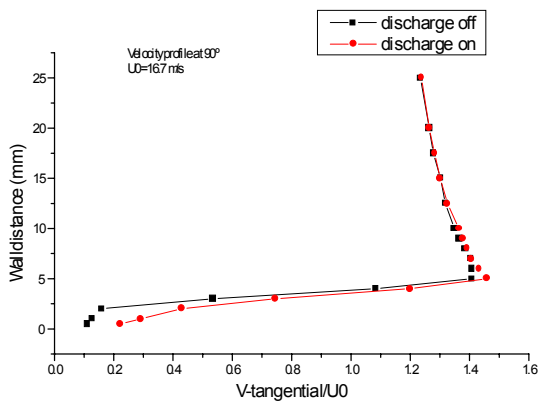


Figure 12c)

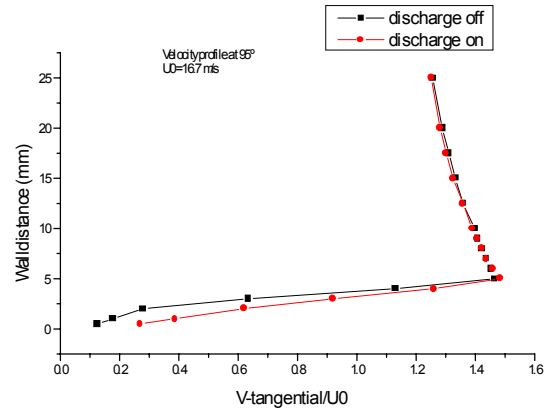


Figure 12 d)

Figure 12: Velocity profile at different angles a)80°, b)85°, c)90°, d)95°. Voltage difference=34kV